Electronic Supplementary Information for

Isotopic substitution affects excited state branching in a DNA duplex in aqueous solution

Yuyuan Zhang,†[a] Kimberly de La Harpe,†[b] Forrest R. Kohl[a] and Bern Kohler*[a]

[a] Department of Chemistry and Biochemistry, The Ohio State University, 100 West 18th Avenue, Columbus, Ohio 43210, United States.
[b] Department of Physics, United States Air Force Academy, U.S. Air Force Academy, Colorado 80840, United States.
† Authors contributed equally to this work.

Experimental Methods

Broadband UV-visible TA

Femtosecond pump pulses at 265 nm were generated by a white light-seeded, two-stage OPA (TOPAS-prime with deep-UV option, Coherent Inc), which was pumped by 1.8 mJ of 800 nm fundamental from a Ti:Sapphire regenerative amplifier (Astrella, Coherent Inc.) that produced 7.5 mJ, 90 fs pulses at a repetition rate of 1 kHz. The pump beam was attenuated to 2μJ / pulse by a variable reflective neutral density filter wheel and focused by a CaF_2 lens to a spot size of 700 μm (fwhm) at the sample.

The white light continuum probe was generated by focusing a small fraction of the 800 nm fundamental (< 1 μJ/pulse) onto a 5-mm thick CaF_2 window (New Light Photonics). Residual fundamental light was removed from the broadband continuum with a 795 nm to 835 nm high reflector (HR795-835HT300-700, Eksma). The broadband continuum beam was collimated by a 90° off-axis parabolic (OAP) mirror with a UV-enhanced aluminum coating (reflective focal length of 50.8 mm). The collimated continuum beam was separated into signal and reference portions using a reflective neutral density filter. The signal portion of the beam

was focused onto the sample by a 90° OAP mirror with a reflective focal length of 200 mm. After the sample, the signal beam was recollimated using a CaF_2 lens and directed into a prism spectrograph. The reference portion of the probe beam bypassed the sample and was also directed into the spectrograph, where signal and reference beams were dispersed by an equilateral CaF_2 prism and projected onto two 512×58 element, back-thinned full-frame transfer charge-coupled device (FFT-CCD) image sensors (S7030-0906, Hamamatsu). The prism spectrograph, detectors, and associated control electronics were purchased from Stresing Entwicklungsbüro (Berlin, Germany).

The probe pulse was delayed with respect to the pump pulse, by varying the path length of the 800 nm fundamental prior to continuum generation. An optical chopper operating at 500 Hz blocked every other pump pulse. The pump-probe polarization was set to magic angle (54.7°). All broadband UV-visible TA spectra were corrected for the dispersion of the white light continuum.

The experiments monitoring the ground state bleach recovery at 250 nm were carried out using the same spectrometer. Instead of the broadband continuum probe, a second OPA generates narrowband probe pulses centered at 250 nm with approximately 1.5 nm bandwidth. The collimated OPA output was delayed with respect to the pump pulse by a motorized translation stage, before it was split into the signal and reference portions. Both portions were directed into the prism spectrograph, and illuminated an area consist of approximately 30 × 30 pixels on the CCD detectors. The transient signals obtained from these illuminated pixels were averaged to yield the kinetic traces shown in Figures 2 and S2.

Global fitting of the broadband transient absorption spectra was performed in the Glotaran software package.[1] Nonlinear least squares fitting of the kinetic traces at 250 nm was

performed using the Igor Pro program (Wavemetrics). All uncertainties reported are twice the standard error, corresponding to a 95% confidence interval.

Sample Handling

Approximately 0.23 μmol (amount of single strand) of $d(GC)_9$ lyophilized powder with Na^+ counter ions (Midland Certified Reagent Company) was dissolved in 2.0 mL of the H_2O solution composed of 50 mM $HPO_4^{2-}/H_2PO_4^-$ phosphate buffer and 100 mM NaCl. For the D_2O solution, the same non-deuterated salts and lyophilized $d(GC)_9$ powder were used as above, with D_2O replacing H_2O for the solvent. Based on the concentration of guanosine and cytidine (1 mM each; 4 labile protons for guanosine, 3 for cytidine) and the phosphate buffer (50 mM, 3 labile protons), we estimated that the H/D ratio in the D_2O solution is approximately 1:700. The solutions were annealed at 90 °C for 10 minutes and then allowed to slowly cooled down to room temperature over a 30-minute period before TA experiments. Temperature-dependent UV-visible and exciton-coupled circular dichroism (ECCD) spectra were recorded prior to the TA experiments. ECCD spectrum confirms that the duplex adopts a B-form geometry (see panels b and d of Figure S1). Melting curves obtained from the absorbance at 278 nm and the CD signal at 250 nm indicate a duplex melting point above 70 °C (panels e and f in Figure S1).

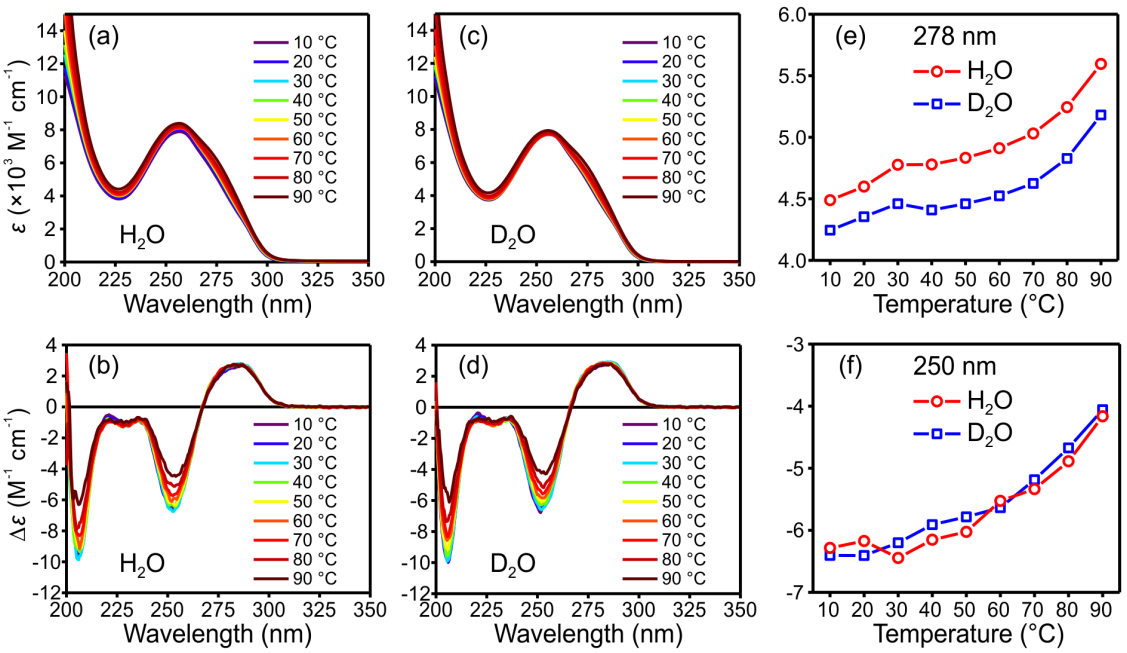

Figure S1. UV-visible absorption spectra (a, c) and circular dichroism (CD) spectra (b, d) of $d(GC)_9 \cdot d(GC)_9$ in buffered H_2O (a, b) and D_2O (c, d), and melting curves determined from the UV-visible spectra at 278 nm (e) and those from the CD spectra at 250 nm (f). The extinction coefficients (ε) in panels a, c, e were calculated using $\varepsilon = A / cL$, where A is the absorbance, c is the concentration per nucleotide, L is the optical path length (1 mm). CD signals ($\Delta\varepsilon$) in panels b, d and f were calculated using $\Delta\varepsilon = \theta_{CD} / (32.98 \text{ deg} \cdot cL)$, where θ_{CD} is the CD signal in degree, c is the concentration per nucleotide, and L is the optical path length (1 mm).

The 2.0 mL solution was circulated through a 500 μm path length flow cell (Harrick) with a 1.0 mm-thick front and a 2.0 mm-thick back window (CaF_2; Photop). The thinner front window was used to minimize dispersion of the deep-UV pump and the UV-visible probe. All measurements were carried out at room temperature.

Using the duplex concentration and excitation conditions stated above, the number of excited states per duplex was estimated as follows. There were approximately 6.8×10^{12} duplexes in the interaction region, which is approximated by a cylinder of length l = 500 μm (path length of the flow cell) and radius r = 350 μm (radius of the pump spot). The number of

absorbed photons was approximately 2.4×10^{12}. Assuming that one absorbed photon leads to one excitation, the number of excitations per duplex is estimated to be 0.4.

Analysis of Ground-State Bleach Recovery Kinetics

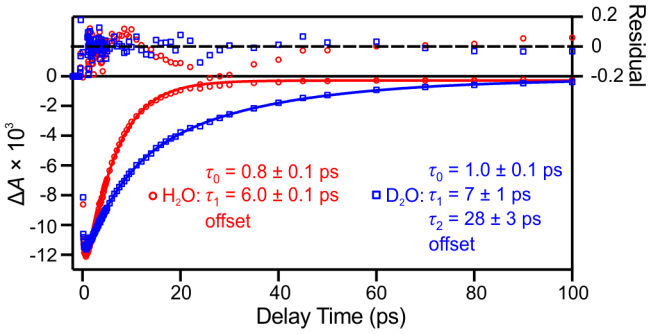

Figure S2. Ground-state bleach recovery kinetic traces monitored at 250 nm following 265 nm excitation of the $d(GC)_9 \cdot d(GC)_9$ duplex in H_2O (red) and in D_2O (blue). The data points are identical to ones shown in Figure 2 of the main text. The D_2O trace was fit to eq. 1; the H_2O trace was fit to the same equation, holding A_2 equal to zero. The fit parameters are included for convenience, and the fit residuals are shown at the top of the panel.

Table S1. Fit parameters for ground-state bleach recovery kinetics traces (1 ps – 500 ps) monitored at 250 nm following 265 nm excitation of the $d(GC)_9 \cdot d(GC)_9$ duplex in H_2O and D_2O.[a]

	A_0	τ_0 (ps)	A_1	τ_1 (ps)	A_2	τ_2 (ps)	A_3
H_2O	6.1	1.3 ± 0.3	–16.4	4.9 ± 0.4	–1.1	25 ± 10	–0.2
D_2O	2.0	1.0 ± 0.4	–5.9	7.0 ± 1.0	–7.0	28 ± 3	–0.2
$A_{i,D}/A_{i,H}$	0.33		0.36		6.4		1

[a] Traces were fit to $\Delta A(t) = A_0\exp(-t/\tau_0) + A_1\exp(-t/\tau_1) + A_2\exp(-t/\tau_2) + A_3$. A_i shown in Table S1 are absolute amplitudes of the measured kinetic traces.

Table S2. Fit parameters for ground-state bleach recovery kinetics traces (1 ps – 500 ps) monitored at 250 nm following 265 nm excitation of the $d(GC)_9 \cdot d(GC)_9$ duplex in H_2O using a different fitting model for the H_2O trace.[a]

	A_0	τ_0	A_1	τ_1	A_2	τ_2	A_3
H_2O	6.4	0.8 ± 0.1	–15.8	6.0 ± 0.1	=0	–	–0.3

[a] Traces was fit to $\Delta A(t) = A_0\exp(-t/\tau_0) + A_1\exp(-t/\tau_1) + A_2\exp(-t/\tau_2) + A_3$. A_2 was set to 0 for the H_2O trace. A_i shown in Table S2 are absolute amplitudes of the measured kinetic traces.

Transient Absorption Spectra of the Monomer Solutions

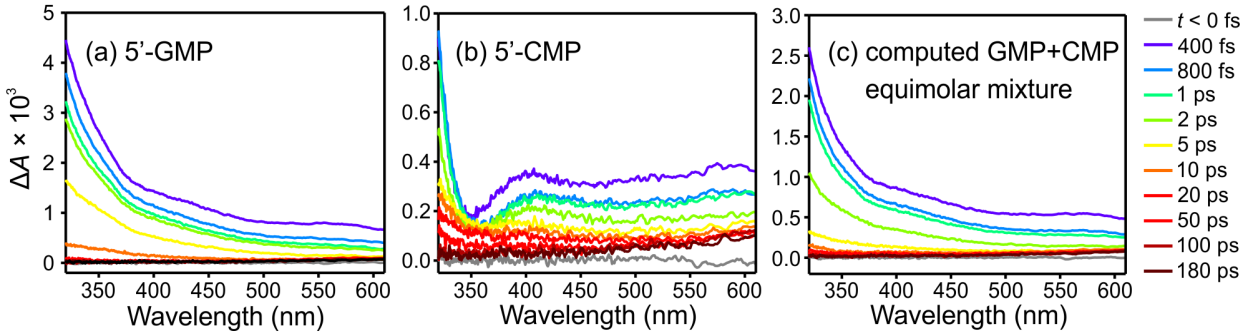

Figure S3. Broadband UV-visible TA spectra of 1.7 mM 5'-GMP (a) and 1.7 mM 5'-CMP (b) in buffered H_2O solutions at selected delay time after 265 nm excitation. These spectra were obtained sequentially with the broadband UV-visible TA spectra of $d(GC)_9 \cdot d(GC)_9$ in buffered H_2O and D_2O solutions (data shown in Figure 3 of the main text), using identical excitation conditions. (c) broadband UV-visible TA spectra for 0.85 mM 5'-GMP and 0.85 mM 5'-CMP mixture, computed from data in panels (a) and (b), and weighted by the difference of molar absorptivity at 265 nm ($\varepsilon_{5'\text{-GMP}}/\varepsilon_{5'\text{-CMP}} = 1.1$). Note that the computed spectrum closely resembles the 5'-GMP spectrum because the signal from 5'-CMP is much weaker.

Spectral Signature of Guanine Radicals

In order to identify the origin of the 390 nm band observed in the broadband UV-visible TA spectra, two-photon ionization of GMP in H_2O at neutral pH (pH = 7.0) was carried out to obtain the absorption spectrum of the guanine radical cation ($G^{\bullet+}$). In addition, photodetached N1-deprotonated GMP ($G(-H)^-$), prepared by dissolving GMP in a basic H_2O solution (pH = 12.0), was used to obtain signatures of the guanine neutral radical ($G(-H)^{\bullet}$). Figure S4 presents

the broadband UV-visible spectra after two-photon excitation of GMP in H_2O at neutral (a) and basic pH (b) at 50 ps, a delay time long enough that any S_1 population has completely decayed. The p*K*a of $G^{\bullet+}$ is 3.9[2], which implies that $G^{\bullet+}$ will deprotonate to $G(-H)^{\bullet}$, while $G(-H)^{-}$ will be stable at neutral pH at equilibrium. However, because estimates of the rate of deprotonation of $G^{\bullet+}$ range from 10^5 s^{-1} to 10^7 s^{-1},[2-3] only the radical cation $G^{\bullet+}$ will be present 50 ps after 2-photon ionization of G.

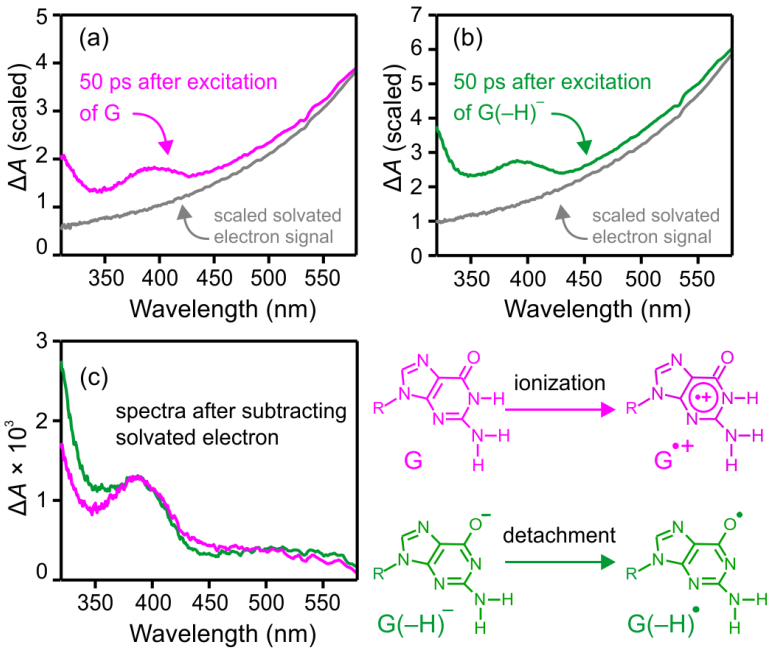

Figure S4. Broadband UV-visible spectra of 5'-GMP in pH = 7.0 (a) and pH = 12.0 (b) H_2O solutions, 50 ps after 265 nm excitation. The solvated electron signal (gray trace) was obtained under identical experimental condition and scaled for ease of comparison. The spectra after subtraction are shown in (c). See text for details on the subtraction procedure.

The absorption spectra in Figure S4 show a similar band at 390 nm with rising absorption at both shorter and longer wavelengths. The long wavelength signal matches well with the absorption spectrum of the solvated electron recorded from neat water with the same instrumentation. For ease of comparison, the solvated electron signal obtained from 2-photon

ionization of pure H_2O is scaled such that all ΔA signal from 320 nm to 580 nm are below that of the G and $G(-H)^-$ at 50 ps after excitation (gray traces in panels a and b of Figure S4). Figure S4c shows the G and $G(-H)^-$ signal after subtraction of the scaled solvated electron signal. Because it is difficult to determine the exact scaling factor, the spectra after correcting for solvated electron are necessarily uncertain. Nevertheless, both spectra are in good agreement with the spectra of $G^{\bullet+}$ and $G(-H)^{\bullet}$ obtained from pulse radiolysis experiments by Candeias and Steenken[2] and accurately capture the distinct feature at 390 nm due to radical absorption.

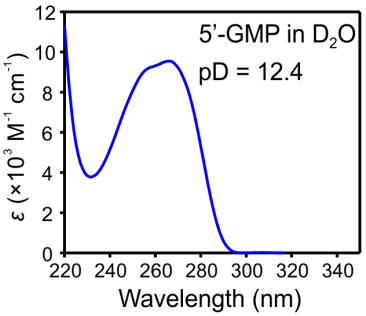

Figure S5. UV-visible absorption spectrum of 5'-GMP in D_2O. The pD (pD = pH + 0.4) of the solution was adjusted to 12.4 by adding dropwise of NaOD solution (Sigma-Aldrich). The extinction coefficients (ε) were calculated using $\varepsilon = A / cL$, where A is the absorbance, c is the nucleotide concentration (10 mM), L is the optical path length (100 μm).

References

1. Snellenburg, J. J.; Laptenok, S. P.; Seger, R.; Mullen, K. M.; van Stokkum, I. H. M., Glotaran: A Java-Based Graphical User Interface for the R Package TIMP. *J. Stat. Softw.* **2012,** *49* (3), 1-22.

2. Candeias, L. P.; Steenken, S., Structure and Acid-Base Properties of One-Electron-Oxidized Deoxyguanosine, Guanosine, and 1-Methylguanosine. *J. Am. Chem. Soc.* **1989,** *111* (3), 1094-1099.

3. Kobayashi, K.; Tagawa, S., Direct Observation of Guanine Radical Cation Deprotonation in Duplex DNA Using Pulse Radiolysis. *J. Am. Chem. Soc.* **2003,** *125* (34), 10213-10218.